

Tissue-specific alternative splicing and the functional differentiation of LmLPM015-1 in Locusta migratoria

Lin Kong

Dalian University of Technology

Huiying Hu

Dalian University of Technology

Pengfei Li

Dalian University of Technology

Mingbo Qu

mingboqu@dlut.edu.cn

Dalian University of Technology

Research Article

Keywords: alternative splicing, chitin, lytic polysaccharide monooxygenases, intestines, tracheal, Locusta migratoria

Posted Date: May 6th, 2024

DOI: https://doi.org/10.21203/rs.3.rs-4310157/v1

License: © 1 This work is licensed under a Creative Commons Attribution 4.0 International License.

Read Full License

Additional Declarations: No competing interests reported.

Abstract

Insect lytic polysaccharide monooxygenases (LPMO15s) are newly discovered copper-dependent enzymes that promote chitin degradation through oxidative cleavage of glycosidic bonds. They are potential pesticide targets due to their critical role for chitin turnover in the integument, trachea, and peritrophic matrix of the midgut during insect molting. However, the knowledge about whether and how LPMOs participate in the chitin turnover in other tissues is still insufficient. Here, using the orthopteran pest Locusta migratoria as a model, a novel alternative splicing site of LmLPM015-1 was discovered and it produces two variants, LmLPM015-1a and LmLPM015-1b. The transcripts of LmLPM015-1a and LmLPMO15-1b were specifically expressed in the trachea and foregut, respectively. RNAi targeting LmLPMO15-1 (a common fragment shared by both LmLPMO15-1a and LmLPMO15-1b), a specific region of LmLPM015-1a or LmLPM015-1b all significantly reduced survival rate of nymphs and induced lethal phenotypes with developmental stasis or molt failure. Ultrastructure analysis demonstrated that LmLPMO15-1b was specifically involved in foregut old cuticle degradation, while LmLPMO15-1a was exclusively responsible for the degradation of the tracheal old cuticle. This study revealed the LmLPMO15-1 achieved tissue-specific functional differentiation through alternative splicing, and proved the significance of the spliced variants during insect growth and development. It provides new strategies for pest control targeting *LPMO15-1*.

Key Message

The LPMO15-1 gene in L. migratoria produced two alternative splicing variants named LmLPMO15-1a and LmLPMO15-1b.

RNAi targeting *LmLPMO15-1a* or *LmLPMO15-1b* all significantly reduced the survival rate of nymphs and induced lethal phenotypes characterized by developmental arrest or molting failure.

LmLPMO15-1a and *LmLPMO15-1b* exhibited tissue-specificity and they are critical for the degradation of old cuticles in the trachea and foregut, respectively.

This study not only provides an example to demonstrate how insect achieves chitin turnover in various tissues through alternative splicing but also imparts potential targets of great promise for future pesticide design.

Introduction

Chitin is well known as an essential structure component of the exoskeletons (Yu et al., 2016; Noh et al., 2018; Qu *et al.*, 2022a; Long et al., 2023), the wings (Xu et al., 2020), the peritrophic membrane of the midgut (Liu et al., 2012; Qu *et al.*, 2022b), the intestinal lining of foregut (Zhang et al., 2021; Yu et al., 2024) and hindgut (Zhang et al., 2021), the taenidia of trachea (Yu et al., 2016; Qu *et al.*, 2022a), as well as in the lumen of salivary glands (De Giorgio et al., 2023). It protects insects from various damages present in their living environment, such as chemical attacks, physical wear and tear, and pathogen

invasion (Merzendorfer & Zimoch., 2003; Muthukrishnan et al., 2012; Zhu et al., 2016). Meanwhile, the rigid structure of chitin also restricts the growth of insects, so chitin is periodically synthesized and degraded during molting (Tetreau et al., 2015; Zhu et al., 2016). The enzymes that participate in the turnover of chitin are crucial for insect development, thus they are potential targets for designing ecofriendly pesticides (Shi et al., 2016; Chen & Yang., 2020; Chen et al., 2020; Liu et al., 2024).

The physiological significance of many enzymes associated with chitin turnover in insects has been extensively studied, such as chitin synthases (CHS) (Qu & Yang., 2011; Qu & Yang., 2012; Long et al., 2023) that are essential for the final step of chitin biosynthesis, chitin deacetylases (CDA) (Arakane et al., 2009; Yu et al., 2016) that participate in chitin modification, Lytic polysaccharide monooxygenases (LPMO) (Qu et al., 2022a; Qu et al., 2022b), chitinases (Cht) (Kramer et al., 1997; Li et al., 2015; Zhang et al., 2018; Zhu et al., 2019; Qu et al., 2021; Zhang et al., 2022; Li et al., 2024) and beta-Nacetylglucosaminidases (Hex) (Rong et al., 2013) that are in charge of chitin degradation. Insects usually encode multiple genes for each enzyme to fulfill their functions in different tissues. Take Locusta migratoria as an example, it encodes two CHSes (CHS1 and CHS2, also known as CHSA and CHSB), four CDAs, three LPMOs, fourteen chitinases, and four Hexes. Some of these genes possess alternative spliced variants to further accomplish their functions in different tissues. *LmCHS1* contains two spliced variants *LmCHS1A* and *LmCHS1B*. *LmCHS1A* is mainly expressed in the integument while *LmCHS1B* is mainly expressed in the trachea. Both variants were proved to be essential for molting during the development of *L. migratoria* (Zhang et al., 2010). This alternative splicing is highly conserved in other insect species such as Tribolium castaneum (Arakane et al., 2004), Anopheles gambiae (Zhang et al., 2013), Sogatella furcifera (Wang et al., 2019). In lepidopteran CHSAs such as OfCHSA from Ostrinia furnacalis, there is an additional splicing site at the 5' region (OfCHSA-2a and OfCHSA-2b), which enables OfCHSA to produce four different transcripts (Qu & Yang., 2011). These transcripts were proved to be differently regulated during development (Qu & Yang., 2012). The BmCHSA-2b from Bombyx mori was proved to be specifically required for pupal wing development (Xu et al., 2017). *LmCDA2* also contains two splice variants LmCDA2a and LmCDA2b. The variant LmCDA2a is essential for molting, whereas *LmCDA2b* seems to be dispensable for survival, although the expression patterns of *LmCDA2a* and LmCDA2b are similar (Yu et al., 2016). TcCDA2 from T. castaneum also has two selectively spliced transcripts, TcCDA2a and TcCDA2b, which appear to have different functions. TcCDA2a is needed for the establishment of the soft fermoraltibial joint cuticle, while TcCDA2b is involved in the formation of the hard elytra (Arakane et al., 2009). This splicing site is conserved in other insect CDA2 genes. Alternative splicing of chitinases has not been extensively investigated in insects. It is only reported in group IV chitinases from Locusta migratoria (Zhang et al., 2022), Bombyx mori (Abdel-Banat et al., 2002), and Lutzomyia longipalpis (Ortigão-Farias et al., 2018).

Lytic polysaccharide monooxygenases (LPMOs) are recently discovered copper-dependent enzymes that oxidatively cleave glycosidic bonds in polysaccharides such as cellulose, chitin, starch, xylan, and pectin (Vaaje-Kolstad et al., 2010; Couturier et al., 2018; Forsberg et al., 2019; Sabbadin et al., 2021). They provide additional attackable sites for glycosyl hydrolases (Couturier et al., 2018; Forsberg et al., 2019; Sabbadin et al., 2021), thus promoting the degradation of polysaccharides (Tandrup et al., 2018;

Jagadeeswaran et al, 2021). They are categorized as members of the auxiliary activities (AA) family members in the Carbohydrate-Active enZymes (CAZy) database, belonging to AA9- AA11 and AA13-AA17. In the realm of insects, LPMOs are specifically classified within the AA15 (LPMO15) family (Sabbadin et al., 2018). They have been identified in *Thermobia domestica* (Sabbadin et al., 2018), Drosophila melanogaster (Zhu et al., 2008), Coptotermes gestroi (Franco Cairo et al., 2020), Tribolium castaneum (Qu et al., 2022a), L. migratoria (Qu et al., 2022a; Qu et al., 2022b), and Bombyx mori (Dong et al, 2016). Phylogenetically, insect LPMO15s can be categorized into four distinct groups, encompassing group \(\text{through group } \(\text{N}. \) So far, the physiological significances of insect LPMO15s have only been investigated in L. migratoria and T. castaneum. In L. migratoria, three LmLPM015s have been classified into group \mathbb{Q} (LmLPM015-1), group \mathbb{Q} (LmLPM015-2), and group \mathbb{Q} (LmLPM015-3) respectively (Qu et al., 2022a; Qu et al., 2022b). LmLPM015-1 exhibits predominant expression within the trachea and epidermis. Its deficiency induced by RNAi leads to developmental stagnation and molting disruption in L migratoria. Transmission electron microscopy (TEM) analysis further elucidated its indispensable role in the degradation of the old cuticle during molting. *LmLPMO15-3* has been proven to be mainly expressed in the midgut and participates in the degradation of the peritrophic matrix (Qu et al., 2022b). In T. castaneum, TcLPM015-1 has been revealed to be pivotal in the degradation of chitin within the old cuticle and trachea during molting (Qu et al., 2022a). However, the knowledge about whether and how LPMOs participate in the turnover of chitin in other tissues is still insufficient.

In this study, alternative splicing of *LmLPMO15-1* was discovered from the orthopteran pest *Locusta migratoria*, which generates two alternative spliced variants namely *LmLPMO15-1a* and *LmLPMO15-1b*. *LmLPMO15-1a* and *LmLPMO15-1b* were highly expressed in the trachea and foregut, respectively. They were proved to possess critical functions with tissue specificity by RNAi in combination with ultrastructure analysis. This work not only deepens our knowledge about the physiological functions of *LPMO15*s in multiple tissues during insect development but also imparts potential targets of great promise for future pesticide design.

Materials and methods

Insects

The eggs of *L. migratoria* were purchased from *L. migratoria* Breeding Co., Ltd., Cangzhou City, Hebei Province, China. They were reared with fresh wheat sprouts in the laboratory at $30 \pm 2^{\circ}$ C and $40 \pm 10^{\circ}$ relative humidity (RH) under 14 h light / 10 h dark cycles.

Identification and analysis of LmLPMO15-1a and LmLPMO15-1b sequences

Putative LmLPMO15-1a and LmLPMO15-1b cDNA sequences were retrieved by performing a BLAST search of the L. migratoria transcriptomes using the sequence of LmLPMO15-1 (GenBank accession number: MZ440879) as a query. To clone the cDNA of LmLPMO15-1a and LmLPMO15-1b, total RNA was isolated from the fifth instar day-1 nymphs by using RNAiso^m Plus (TaKaRa, China). 1 μ g of total RNA

was used to prepare cDNA using the PrimeScript^T 1st Strand cDNA Synthesis Kit (TaKaRa, China) according to the instructions of the manufacturer. The 5' sequences of both *LmLPMO15-1a* and *LmLPMO15-1b* were obtained by PCR amplification using the gene-specific primers shown in Supplementary Table S1. The PCR products were cloned into the pEASY-T1 vector (TransGen Biotech, Beijing, China) and sequenced (Sangon Biotech, Changchun, China). After sequencing, the sequence of *LmLPMO15-1a* was proved to be the same as the *LmLPMO15-1* sequence previously obtained by our laboratory. While the sequence of *LmLPMO15-1b* was proved to be different. Then the 3' sequence of *LmLPMO15-1b* was amplified by 3'-RACE using SMARTer® RACE 5' / 3' Kit (TaKaRa, USA) according to the user manual. The products of 3'-RACE including the full open reading frame were cloned into the pEASY-T1 vector (TransGen Biotech, Beijing, China), and sequenced (Sangon Biotech, Changchun, China). The full gene sequence including the 5' and 3' UTR of *LmLPMO15-1b* was deposited in the National Center for Biotechnology Information (NCBI) (GenBank accession number: PP461030).

Bioinformatic analysis

The gene structure was determined by searching the *L. migratoria* genome in NCBI using the cDNA sequences of *LmLPMO15-1a* and *LmLPMO15-1b* as queries. Exons and introns were identified by comparing genomic DNA and cDNA sequences, and the GT-AG rule was applied to determine exon and intron boundaries, and then plotted. The 2kb upstream sequence of *LmLPMO15-1a* and *LmLPMO15-1b* genes were obtained from the genome of *L. migratoria* in NCBI, respectively. Then, the promoter sequence was analyzed by the NNPP program of the Berkeley Drosophila Genome Project (https://www.bdgp.org/seq_tools/nnppHelp.html).

The cDNA sequences of *LmLPMO15-1a* and *LmLPMO15-1b* were translated using the translation tools at ExPASy (http://www.expasy.org/tools/dna.html). LPMO15 homologs of *LmLPMO15-1a* and *LmLPMO15-1b* from other insect species were searched using BLASTP against genomes or transcriptomes in the NCBI database, respectively. A total of 14 amino acid sequences of LPMO15 were identified (Table S2). SignalP 5.0 (https://services.healthtech.dtu.dk/services/SignalP-5.0/) was used to predict signal peptides. The deduced protein domains were determined by SMART (http://smart.embl-heidelberg.de/). Multiple amino acid sequence alignments were performed using Clustal Omega (https://www.ebi.ac.uk/Tools/msa/clustalo/). Phylogenetic trees were constructed using the signal peptide sequences by the neighbour-joining (NJ) method via MEGA 11.0 software. Bootstrap analysis was performed with 1000 replications using a cut off of 50% similarity.

Tissue- and stage-specific expression analysis of LmLPMO15-1a and LmLPMO15-1b

To detect the tissue-specific gene expression pattern, the foregut (Fg), midgut (Mg), hindgut (Hg), trachea (Tr), Malpighian tubules (MT), epidermis (Ep), and gastric caecum (GC) were dissected from the fifth instar day-3 nymphs. To detect the stage-specific expression pattern, the fourth instar day-2 (N4D2), fourth instar day-4 (N4D4), fourth instar day-6 (N4D6), fifth instar day-2 (N5D2), fifth instar day-4 nymph (N5D4), fifth instar day-6 (N5D6), fifth instar day-8 (N5D8) nymphs, and day-2 (A2), day-4 (A4), day-6 (A6) adults were collected. Total RNA extraction and cDNA synthesis from these samples were performed as

previously described. The Real-time PCR Detection System LightCycler480II (Roche, Basel, Switzerland) was used to perform quantitative reverse-transcription PCR (RT-qPCR) in a 20 μ L reaction volume comprising 10 μ L MonAmp TM Chemo Hs qPCR Mix (Monad, Shanghai, China), 1 μ L complementary DNA (cDNA) as the template, and 0.2 μ mol/L of each primer. Ribosomal protein 49 (*Rp49*) from *L. migratoria* (*LmRp49*) was used as an endogenous control. Each sample included three biological replicates and three technical replicates. The relative expression levels for each gene were calculated relative to those of the reference gene according to the $2^{-\Delta\Delta Ct}$ method (Qu et al., 2021). The genespecific qPCR primers used to detect the expression patterns of the *LmLPM015-1a* and *LmLPM015-1b* genes are listed in Table S1.

RNAi of LmLPMO15-1a and LmLPMO15-1b in L. migratoria by dsRNA injection

The variable sequences at the 5' end of *LmLPMO15-1a* and *LmLPMO15-1b* were selected for specific double-stranded RNA (ds*LmLPMO15-1a*, ds*LmLPMO14-1b*) synthesis, to interfere with the expression of *LmLPMO15-1a* and *LmLPMO15-1b* respectively. The common sequence of *LmLPMO15-1a* and *LmLPMO15-1b* was selected for specific double-stranded RNA (ds*LmLPMO15-1*) synthesis, to interfere with the expression of both *LmLPMO15-1a* and *LmLPMO15-1b* genes, and ds*GFP* was used as a negative control.

The pEASY-T1 vector carrying the *LmLPMO15-1a* and *LmLPMO15-1b* genes was used as a template to amplify PCR products for the synthesis of ds*LmLPMO15-1a*, ds*LmLPMO14-1b*, and ds*LmLPMO15-1*. The T7 RNA promoter sequences were added in the 5' end of the PCR primers (Table S1). dsRNAs were synthesized using the T7 RiboMAXTM Express RNAi System (Promega, Madison, WI, USA), according to instructions of the manufacturer using the PCR products as a template.

10 µg of ds*LmLPMO15-1*, ds*LmLPMO15-1a*, ds*LmLPMO15-1b*, and ds*GFP* were injected into the penultimate abdominal segment of the fifth instar day-3 nymphs, respectively. An equal amount of dsRNA was injected again to strengthen the RNAi efficiency after 48 h. Total RNA was extracted after 72 h, and then the gene expression levels were examined by qRT-PCR. The dsRNA of each gene was injected into 40 nymphs, 10 nymphs for detecting interference efficiency and ultrastructure analysis, and 30 nymphs for observing morphological changes during development. The visible phenotypes were observed daily until the nymphs molted into adults.

Ultrastructure analysis of foregut, and trachea after RNAi

The nymphs from ds LmLPMO15-1, ds LmLPMO15-1a, ds LmLPMO15-1b, and ds GFP injected groups were collected and dissected on the fifth instar day-8 nymphs (before molting), respectively. The dissected foregut and hindgut were fixed in 4% paraformaldehyde for 24 hours, dehydrated in a graded ethanol series (30%, 50%, 70%, 90%, and 100%) for 30 min each, and then embedded in paraffin. 5 μ m paraffin sections were prepared and stained with hematoxylin and eosin (H&E) staining. For better visualization of chitin in the foregut, the nuclei and chitin were stained using DAPI and Fluorescent Brightener 28, respectively. After staining, the foregut sections were imaged using an Olympus IX-83

Inverted Fluorescence Microscope. The ultrastructure of the trachea from the dsRNA-treated fifth instar day-8 nymphs was analyzed by transmission electron microscopy (TEM). TEM analyses were performed according to previously described methods (Qu *et al.*, 2022a) and images were captured with a HITACHI HT7800 transmission electron microscope (TEM, Japan).

Results

Identification and characterization of LmLPMO15-1a and LmLPMO15-1b

One novel transcript (GenBank accession number: PP461030) encoding LmLPM015-1 was identified from the transcriptome database of L. migratoria in NCBI, which encoded a peptide fragment with the same C-terminal regions but different N-terminal regions as the previously identified LmLPM015-1 (GenBank accession number: MZ440879). Thus the previous transcript was defined as LmLPM015-1a, while the new transcript was defined as *LmLPMO15-1b*. To obtain the full open reading frame of LmLPMO15-1b, 3' RACE was performed (Fig. S1), and a 1675 bp transcript was obtained. Like LmLPMO15-1a, LmLPMO15-1b also possessed an open reading frame of 1017 bp and encoded 339 amino acids with a signal peptide at the N-terminus. To investigate whether these two transcripts were generated by gene splicing, the genomic structure of LmLPMO15 was then analyzed by comparing its genomic DNA with the cDNA sequences. The total gene of LmLPMO15 was discovered to contain 14 exons. The transcript of *LmLPMO15-1b* was produced when exons 1–10 were transcript, while the LmLPMO15-1a transcript included sequences from exons 11–14 and 4–10 in the 5' to 3' direction (Fig. 1A). They shared the same exons 4–10 and alternative splicing occurs in exons 11–14 of LmLPM015-1a and exons 1-3 of LmLPM015-1b. In addition, two promoters were predicted based on genome sequence analysis. One (promoter a) is located between exon 10 and exon 11, and it may promote the transcription of LmLPMO15-1a. Another one (promoter b) is located upstream of exon 1, and it may promote the transcription of LmLPMO15-1b (Fig. 1A). The genome sequence analysis of LmLPMO15-1 indicated that the regulation of these two transcripts was complicated during insect development.

To investigate whether this alternative splicing of *LmLPMO15-1* was widely distributed in other insects, BLASTP was performed to search identical sequences to *LmLPMO15-1a* or *LmLPMO15-1b* against genomes and transcriptomes in the NCBI database. These alternatively spliced sequences were only found in orthoptera, such as *Schistocerca americana* and *Schistocerca nitens*. The full lengths of these proteins all contain one signal peptide, one AA15 domain, and two internal repeats rich in cysteine residues at the C-terminal end. In each species, both spliced variants shared the same C-terminal amino acid sequence and differed only in the signal peptide (Fig. 1B). This splicing pattern is highly conserved in orthoptera insects. Then a phylogenetic tree was constructed using only the signal peptide sequences (encoded by the spliced exons) in these sequences. The results showed that all LPMO15-1a and LPMO15-1b isoforms were collectively categorized into two separate branches, which indicated an early divergence of two distinct LPMO15-1 variants (Fig. 1C).

Stage- and tissue-specific expression analysis of LmLPMO15-1a and LmLPMO15-1b

To investigate the possible functions of *LmLPMO15-1a* and *LmLPMO15-1b* during the development of *L. migratoria*, the stage-specific expression patterns of *LmLPMO15-1a* and *LmLPMO15-1b* were first examined from the fourth instar day-2 nymph (N4D2) to adults. The results demonstrated that the expression of *LmLPMO15-1a* was up-regulated at stages N4D2 and N5D2-N5D4 after molting, and was also slightly up-regulated at A6 (Fig. 2A). The expression level of *LmLPMO15-1b* was up-regulated at N4D4 and N5D8 (Fig. 2B). Then, their gene expression patterns were analyzed in different tissues, including the foregut, midgut, hindgut, trachea, malpighian tubules, epidermis, and gastric caecum. The expression level of *LmLPMO15-1a* was highest in the trachea, and was higher in the foregut and epidermis than in the midgut, hindgut, malpighian tubules, and gastric caecum (Fig. 2C). The expression level of *LmLPMO15-1b* was significantly higher in the foregut than that in the midgut, hindgut, malpighian tubules, and epidermis, and its transcripts were barely detectable in the gastric caecum (Fig. 2D). The expression patterns of *LmLPMO15-1a* and *LmLPMO15-1b* suggested that *LmLPMO15-1a* may function in the trachea during development, whereas *LmLPMO15-1b* may play a role in the foregut during molting.

Phenotypes of L. migratoria caused by LmLPM015-1a or LmLPM015-1b specific RNAi

To further explore the functions of *LmLPMO15-1* and its two spliced variants during insect development, their expression were inhibited by dsRNA injection targeting *LmLPMO15-1*, *LmLPMO15-1a*, and *LmLPMO15-1b*, respectively. The double-stranded green fluorescent protein gene (ds *GFP*) was used as a control. The gene silencing efficiency was first verified by RT-qPCR measurement, and the results showed that the expression levels of *LmLPMO15-1* in ds *LmLPMO15-1*, ds *LmLPMO15-1a* and ds *LmLPMO15-1b* injection groups were significantly lower than that in the ds *GFP* group, with silencing efficiencies of 91.36%, 70.89% and 45.89%, respectively (Fig. 3A). The expression level of *LmLPMO15-1a* in the ds *LmLPMO15-1a* injection group were significantly lower than those in the ds *GFP* injection group, with silencing efficiencies of 57.29% and 63.53%, respectively, whereas there was no significant change in the ds *LmLPMO15-1b* injection group (Fig. 3B). The expression level of *LmLPMO15-1b* was significantly lower in the ds *LmLPMO15-1*, and ds *LmLPMO15-1b* injection groups than that in the ds *GFP* injection group, with silencing efficiencies of 98.02% and 98.52%, respectively, while its expression level in the ds *LmLPMO15-1a* injection group showed no significant change (Fig. 3C). These results indicated that the transcripts down regulation by the injection of corresponding dsRNAs of *LmLPMO15-1a*, and *LmLPMO15-1b* were efficient and specific.

The phenotypes caused by the dsRNA injection were then observed. In the ds*GFP*-injection group, all the nymphs survived (Fig. 3D) and began to molt to adults at N5D6 with a final eclosion rate of 100% (Fig. 3E). The nymphs injected with ds*LmLPMO15-1*, ds*LmLPMO15-1a*, or ds*LmLPMO15-1b* began to exhibit lethal phenotype at N5D4 (Fig. 3D) and had much lower eclosion rates compared to that of ds*GFP* injection group (Fig. 3E). In the ds*GFP*-injection group, 100% nymphs were molt to adults (Fig. 3F and 3G-a). After injection of ds*LmLPMO15-1*, 37.5% of nymphs were found arrested at the nymph stage, and these nymphs eventually died before molting (Fig. 3F and 3G-b, P1). A further 25% of nymphs showed a

lethal phenotype during molting, with 10% of nymphs exhibiting a just-expanded wing molting failure phenotype (Fig. 3F and 3G-b, P2) and 15% of nymphs exhibiting a more advanced molting failure phenotype (Fig. 3F and 3G-b, P3). The total lethality is 62.5% in the ds*LmLPMO15-1* injection group (Fig. 3F). In the ds*LmLPMO15-1a* injected group, 45% of nymphs died before molting (Fig. 3F and 3G-c, P1) and another 15% of nymphs exhibited a more advanced molting failure phenotype (Fig. Figure 3F and 3G-c, P3). The injection of ds*LmLPMO15-1b* resulted in 37.5% of nymphs died before molting (Fig. 3F and 3G-d, P1), 15% of nymphs showed a just-expanded wing molting failure phenotype (Fig. 3F and 3G-d, P2) and 5% nymphs showed a more advanced molting failure phenotype (Fig. 3F and 3G-d, P3). These results suggested that all the transcripts of *LmLPMO15* played a crucial role during the development of *L. migratoria*.

LmLPMO15-1b plays a crucial role in the degradation of the old foregut cuticle.

Since *LmLPMO15-1b* is highly expressed in the foregut, H&E staining was performed to further observe the changes in the foregut caused by the RNAi of *LmLPMO15-1* and its two variants. The results showed that the old cuticle of the foregut in the ds *GFP* injection group (control group) was thin and degraded into small pieces dispersed in the intestinal lumen (Fig. 4A), while in the ds *LmLPMO15-1* and ds *LmLPMO15-1b* groups, the old cuticles still maintain the shape with a regular arrangement showing the profile of epithelial cells. In the *dsLmLPMO15-1a* group, the old cuticle was loosely distributed in the intestinal lumen (Fig. 4A). A further measurement of the thickness of the old foregut cuticle demonstrated that the old cuticle in the ds *LmLPMO15-1* or ds *LmLPMO15-1b* injection groups was thicker than that in the ds *GFP* injection group (Fig. 4B), and the thickness in the ds *LmLPMO15-1a* group was lower compared to that in the ds *LmLPMO15-1* or ds *LmLPMO15-1b* groups (Fig. 4B).

To better analyze the changes of the old cuticle in the foregut after RNAi, the sections were stained with FB28 and DAPI to observe the chitin (blue) and nuclei (red), respectively. The results demonstrated that the blue color representing chitin in the old cuticle of ds *GFP* or ds *LmLPMO15-1a* injection groups were weak or even invisible, indicating that the degradation of chitin in the old cuticle was almost completed (Fig. 5). The blue color representing chitin in the old cuticle of ds *LmLPMO15-1* or ds *LmLPMO15-1* groups was bright and in a regular shape, indicating that the degradation of chitin in the old cuticle was inhibited (Fig. 5). In summary, these results demonstrated that the degradation of old cuticle chitin in the foregut of *L. migratoria* during molting is mainly accomplished by *LmLPMO15-1b*.

Degradation of old tracheal cuticle requires LmLPMO15-1a

To further observe the changes in the cuticle structure of the trachea caused by the RNAi of *LmLPMO15-1* and its two variants, transmission electron microscopy was applied due to the small size of the trachea. The results showed that the tracheal cuticles in the ds *GFP* or ds *LmLPMO15-1b* injection group were relatively thin and were degraded into many small pieces and scattered in the tracheal lumen (Fig. 6A). However, in the ds *LmLPMO15-1* or ds *LmLPMO15-1a* injection group, the old tracheal cuticle still maintained the arrangement of taenidia morphology showing the profile of epithelial cells, indicating that the degradation of old tracheal cuticle was inhibited (Fig. 6A). The thickness of the old trachea

cuticle in the ds*LmLPMO15-1* or ds*LmLPMO15-1a* injection group was significantly higher than that in the ds*GFP* or ds*LmLPMO15-1b* injection groups (Fig. 6B). All these results demonstrated that the degradation of the old trachea cuticle during the molting of *L. migratoria* is mainly accomplished by *LmLPMO15-1a*.

Discussion

Insect LPMO15s were newly discovered copper-dependent enzymes that participate in the degradation of chitin through oxidative cleavage of glycosidic bonds during insect development. They are potentially new targets for designing eco-friendly pesticides. Using *L. migratoria* as a model, our previous work has demonstrated the group I gene *LmLPMO15-1* participates in the degradation of chitin in the integument, while the group III gene *LmLPMO15-3* is involved with the turnover of chitin in the midgut (Qu *et al.*, 2022a; Qu *et al.*, 2022b). However, as a critical structure component in insects, chitin is also present in the extracellular matrix of other tissues, such as trachea and foregut. The knowledge about whether and how LPMOs participate in the chitin turnover in these tissues is still insufficient. Here for the first time, we identified the presence of alternative splicing in insect *LPMO15-1s*, using *L. migratoria* as a model. The spliced variants *LmLPMO15-1a* and *LmLPMO15-1b* were proved to be tissue-specific and functional differentiation. It provides a strategy that how insects achieve chitin turnover in different tissues.

Alternative splicing of LPM015-1 in insect

Alternative splicing expands the coding capacity of genes. It has been discovered in many enzymes involved with chitin turnover, such as chitin synthase (Qu & Yang., 2011; Qu & Yang., 2012; Long et al., 2023) and chitin deacetylase (Arakane et al., 2009; Yu et al., 2016). The resulting transcripts were either induced by different promoters or encoded variant protein isoforms. Here a novel alternative splicing site was found in the group I gene *LmLPMO15-1*, which has been proven to participate in cuticular chitin degradation (Qu et al., 2022a). The sequence alignment of the spliced transcripts LmLPM015-1a and LmLPM015-1b reveals that the primary differences between these two alternative splicing variants lie mainly in the 5' region. This difference indicates the two variations contain their promoters (Fig. 1A). The translated sequences of the two alternative splicing variants only differ in the signal peptide, with the mature peptides being identical (Fig. 1B). Therefore, the LPMO proteins produced by alternative splicing should possess the same catalytic properties. All these suggested the main role of alternative splicing is to regulate the expression of *LmLPMO15-1* in different tissues and developmental stages. This splicing pattern is also identified to be highly conserved in other LPMO15-1s from orthopteran insects (Fig. 1B), suggesting it is an orthopteran-specific splicing. In other insect species such as *Bombyx mori*, *Manduca* sexta, Plutella xylostella, and Drosophila melanogaster, alternative splicing of LPM015-1 could also be identified from the NCBI database (Table S3). However, their splicing sites are located in the middle of their transcripts, leading to different mature peptides (Fig. S2). This information indicates different strategies for insects to produce multiple transcripts of LPM015-1 through alternative splicing. However, the functions of these transcripts need to be further investigated.

Functions of spliced variants of LmLPMO15-1 during development.

Previous research in *L. migratoria* demonstrated that downregulation of *LmLPMO15-1* results in lethal phenotypes, primarily characterized by the inability to digest the old chitinous layers in the cuticle (Qu et al., 2022a), while the RNAi of *LmLPMO15-3* hinders the digestion of the peritrophic membrane in the midgut during molting (Qu *et al.*, 2022b). The two alternatively spliced variants *LmLPMO15-1a* and *LmLPMO15-1b* were proved to be primarily expressed in the trachea and foregut respectively (Fig. 2C and 2D), indicating their important roles in these tissues. A further downregulation of these transcripts by RNAi demonstrated that defects in *LmLPMO15-1a* specifically prevent the degradation of the tracheal old chitinous layer (Fig. 6A), clarifying the role of *LmLPMO15-1a* in tracheal chitin digestion, which is consistent with the function of *TcLPMO15-1* in *T. castaneum* (Qu *et al.*, 2022a). Conversely, the absence of *LmLPMO15-1b* specifically fails to degrade the old chitinous layer of the foregut (Fig. 5A), indicating that *LmLPMO15-1b* is primarily responsible for foregut chitin degradation. These results clearly demonstrate a functional differentiation of alternatively spliced transcripts in the trachea and foregut. *L. migratoria* generates a specialized transcript through alternative splicing to fulfill chitin degradation in the trachea and foregut.

Conclusions and perspective

This study reveals, for the first time, the existence of alternative splicing in *LPMO15-1* using *L. migratoria* as a model. The resulting two alternative splicing variants *LmLPMO15-1a* and *LmLPMO15-1b* exhibited tissue-specificity and they were critical for the degradation of old cuticle in trachea and foregut, respectively. This work provides an example to demonstrate how insect achieves chitin turnover in different tissues through alternative splicing. It deepens the understanding of the crucial role of *LPMO15-1* during insect development. These findings will contribute to the development of novel strategies for pest control targeting LPMO enzymes.

Declarations

Funding

This work was supported by the National Natural Science Foundation of China (31872972, 32170501)

Author contributions

MQ supervised the project. MQ and KL designed the research study. Material preparation was performed by LK, HH, and PL. Data collection and analysis were performed by LK and MQ. The first draft of the manuscript was written by LK and MQ, and all authors commented on previous versions of the manuscript. All authors read and approved the final manuscript.

Data availability

The datasets generated during and/or analyzed during the current study are available from the corresponding author upon reasonable request.

Declaration

The authors have no relevant financial or non-financial interests to disclose.

References

- Yu, R., Liu, W., Li, D., Zhao, X., Ding, G., Zhang, M., Ma, E., Zhu, K., Li, S., Moussian, B., & Zhang, J. (2016). Helicoidal Organization of Chitin in the Cuticle of the *Migratory Locust* Requires the Function of the Chitin Deacetylase2 Enzyme (*LmCDA2*). The Journal of Biological Chemistry. 291(47), 24352–24363. https://doi.org/10.1074/jbc.M116.720581
- 2. Noh, M. Y., Muthukrishnan, S., Kramer, K. J., & Arakane, Y. (2018). A chitinase with two catalytic domains is required for organization of the cuticular extracellular matrix of a *beetle*. PLoS genetics. *14*(3), e1007307. https://doi.org/10.1371/journal.pgen.1007307
- 3. Qu Mingbo, Guo Xiaoxi, Tian Suang, Yang Qing, Kim Myeongjin, Mun Seulgi, Noh Mi Young, Kramer Karl J., Muthukrishnan Subbaratnam, Yasuyuki Arakane. (2022a) AA15 lytic polysaccharide monooxygenase is required for efficient chitinous cuticle turnover during insect molting. Communications Biology. 5, 518. https://doi.org/10.1038/s42003-022-03469-8
- 4. Long, G., Liu, X., Guo, H., Zhang, M., Gong, L., Ma, Y., Dewer, Y., Mo, W., Ding, L., Wang, Q., He, M., & He, P. (2023). Oral-based nanoparticle-wrapped dsRNA delivery system: a promising approach for controlling an urban pest, *Blattella germanica*. Journal of Pest Science. 97, 739–755. https://doi.org/10.1007/s10340-023-01677-7
- Xu, G., Yi, Y., Lyu, H., Gong, C., Feng, Q., Song, Q., Peng, X., Liu, L., & Zheng, S. (2020). DNA methylation suppresses chitin degradation and promotes the wing development by inhibiting Bmara-mediated chitinase expression in the *silkworm*, *Bombyx mori*. Epigenetics & chromatin. *13*(1), 34. https://doi.org/10.1186/s13072-020-00356-6
- 6. Liu, X., Zhang, H., Li, S., Zhu, K. Y., Ma, E., & Zhang, J. (2012). Characterization of a midgut-specific chitin synthase gene (*LmCHS2*) responsible for biosynthesis of chitin of peritrophic matrix in *Locusta migratoria*. Insect biochemistry and molecular biology, 42(12), 902–910. https://doi.org/10.1016/j.ibmb.2012.09.002
- 7. Qu Mingbo, Guo Xiaoxi, Kong Lin, Hou Lingjie, Yang Qing. (2022b) A midgut-specific lytic polysaccharide monooxygenase of *Locusta migratoria* is indispensable for the deconstruction of the peritrophic matrix. Insect Science. 0, 1–12. https://doi.org/10.1111/1744-7917.13016
- 8. Zhang, M., Ma, P. J., Zhang, T. T., Gao, Z. M., Zhao, P., Liu, X. J., Zhang, X. Y., Liu, W. M., Yu, R. R., Moussian, B., & Zhang, J. Z. (2021). Roles of LmCDA1 and LmCDA2 in cuticle formation in the

- foregut and hindgut of *Locusta migratoria*. Insect science. *28*(5), 1314–1325. https://doi.org/10.1111/1744-7917.12874
- 9. Yu, R. R., Duan, J. Q., Zhao, X. M., Abbas, M., Zhang, Y. P., Shi, X. K., Chen, N. and Zhang, J. Z. (2024) Knickkopf (LmKnk) is required for chitin organization in the foregut of Locusta migratoria. Insect Science, DOI 10.1111/1744-7917.13313. https://doi.org/10.1111/1744-7917.13313
- 10. De Giorgio, E., Giannios, P., Espinàs, M. L., & Llimargas, M. (2023). A dynamic interplay between chitin synthase and the proteins Expansion/Rebuf reveals that chitin polymerization and translocation are uncoupled in *Drosophila*. PLoS biology. 21(1), e3001978. https://doi.org/10.1371/journal.pbio.3001978
- 11. Merzendorfer, H. and Zimoch, L. (2003) Chitin metabolism in insects: structure, function and regulation of chitin synthases and chitinases. Journal of Experimental Biology. 206, 4393–4412. https://doi.org/10.1242/jeb.00709
- 12. Muthukrishnan, S., Merzendorfer, H., Arakane, Y., & Kramer, K. J. (2012). Chitin metabolism in insects. In *Insect molecular biology and biochemistry* (pp. 193–235). Academic Press.
- 13. Zhu, K.Y., Merzendorfer, H., Zhang, W., Zhang, J. and Muthukrishnan, S. (2016) Biosynthesis, turnover, and functions of chitin in insects. Annual Review of Entomology. 61, 177–196. https://doi.org/10.1146/annurev-ento-010715-023933
- 14. Tetreau, G., Cao, X., Chen, Y. R., Muthukrishnan, S., Jiang, H., Blissard, G. W. *et al.* (2015) Overview of chitin metabolism enzymes in *Manduca sexta*: identification, domain organization, phylogenetic analysis and gene expression. Insect Biochemistry and Molecular Biology. 62, 114–126. https://doi.org/10.1016/j.ibmb.2015.01.006
- 15. Shi, J. F., Mu, L. L., Chen, X., Guo, W. C., & Li, G. Q. (2016). RNA interference of chitin synthase genes inhibits chitin biosynthesis and affects larval performance in *Leptinotarsa decemlineata* (Say). International journal of biological sciences. 12(11), 1319–1331. https://doi.org/10.7150/ijbs.14464
- 16. Chen, W. and Yang, Q. (2020) Development of novel pesticides targeting insect chitinases: a minireview and perspective. Journal of Agricultural and Food Chemistry. 68, 4559–4565. https://doi.org/10.1021/acs.jafc.0c00888
- 17. Chen, W., Jiang, X. and Yang, Q. (2020) Glycoside hydrolase family 18 chitinases: the known and the unknown. Biotechnology Advances. 43, 107553. https://doi.org/10.1016/j.biotechadv.2020.107553
- 18. Liu, X., Liu, H., Wang, Y., Duan, R., Li, S., Qian, L., Chen, F. (2024) Elevated CO2 leads to thick-skinned thrips by altering trehalose and chitin metabolisms. Journal of Pest Science. 97, 951–963. https://doi.org/10.1007/s10340-023-01697-3
- 19. Qu, M., & Yang, Q. (2011). A novel alternative splicing site of class A chitin synthase from the insect *Ostrinia furnacalis* gene organization, expression pattern and physiological significance. Insect biochemistry and molecular biology, 41(12), 923–931. https://doi.org/10.1016/j.ibmb.2011.09.001
- 20. Qu, M., & Yang, Q. (2012). Physiological significance of alternatively spliced exon combinations of the single-copy gene class A chitin synthase in the insect *Ostrinia furnacalis* (Lepidoptera). Insect molecular biology, 21(4), 395–404. https://doi.org/10.1111/j.1365-2583.2012.01145.x

- 21. Arakane, Y., Dixit, R., Begum, K., Park, Y., Specht, C. A., Merzendorfer, H., Kramer, K. J., Muthukrishnan, S., and Beeman, R. W. (2009) Analysis of functions of the chitin deacetylase gene family in *Tribolium castaneum*. Insect biochemistry and molecular biology. 39, 355–365. https://doi.org/10.1016/j.ibmb.2009.02.002
- 22. Kramer, K. J., & Muthukrishnan, S. (1997). Insect chitinases: molecular biology and potential use as biopesticides. Insect biochemistry and molecular biology. *27*(11), 887–900. https://doi.org/10.1016/s0965-1748(97)00078-7
- 23. Li, D., Zhang, J., Wang, Y., Liu, X., Ma, E., Sun, Y., Li, S., Zhu, K. Y., & Zhang, J. (2015). Two chitinase 5 genes from *Locusta migratoria*: molecular characteristics and functional differentiation. Insect biochemistry and molecular biology, 58, 46–54. https://doi.org/10.1016/j.ibmb.2015.01.004
- 24. Zhang, T., Liu, W., Li, D., Gao, L., Ma, E., Zhu, K. Y., Moussian, B., Li, S., & Zhang, J. (2018). *LmCht5-1* promotes pro-nymphal molting during locust embryonic development. *Insect biochemistry and molecular biology*, 101, 124–130. https://doi.org/10.1016/j.ibmb.2018.09.001
- 25. Zhu, B., Shan, J., Li, R., Liang, P., & Gao, X. (2019). Identification and RNAi-based function analysis of chitinase family genes in *diamondback moth*, *Plutella xylostella*. Pest management science. *75*(7), 1951–1961. https://doi.org/10.1002/ps.5308
- 26. Qu, M. B., Sun, S. P., Liu, Y. S., Deng, X. R., Yang, J., & Yang, Q. (2021). Insect group II chitinase *Of*ChtII promotes chitin degradation during larva-pupa molting. Insect Science, 28(3), 692–704. https://doi.org/10.1111/1744-7917.12791
- 27. Zhang, T., Huo, Y., Dong, Q., Liu, W., Gao, L., Zhou, J., Li, D., Zhang, X., Zhang, J., & Zhang, M. (2022). *LmCht5-1* and *LmCht5-2* Promote the Degradation of Serosal and Pro-Nymphal Cuticles during Locust Embryonic Development. *Biology*, 11(12), 1778. https://doi.org/10.3390/biology11121778
- 28. Li, C., Wang, L., Liu, L., Lv, N., Gou, Y., Wang, S., Zhou, J., & Liu, C. (2024). Silencing of *ApCht7* and *ApCht10* revealed their function and evaluation of their potential as RNAi targets in *Acyrthosiphon pisum*. *Journal of Pest Science*. 1–12. https://doi.org/10.1007/s10340-023-01722-5
- 29. Rong, S., Li, D. Q., Zhang, X. Y., Li, S., Zhu, K. Y., Guo, Y. P., Ma, E. B., & Zhang, J. Z. (2013). RNA interference to reveal roles of β-N-acetylglucosaminidase gene during molting process in *Locusta migratoria*. Insect Science, 20(1), 109–119. https://doi.org/10.1111/j.1744-7917.2012.01573.x
- 30. Zhang, J., Liu, X., Zhang, J., Li, D., Sun, Y., Guo, Y., Ma, E., & Zhu, K. Y. (2010). Silencing of two alternative splicing-derived mRNA variants of chitin synthase 1 gene by RNAi is lethal to the oriental migratory locust, *Locusta migratoria manilensis* (Meyen). Insect biochemistry and molecular biology, 40(11), 824–833. https://doi.org/10.1016/j.ibmb.2010.08.001
- 31. Arakane, Y., Hogenkamp, D. G., Zhu, Y. C., Kramer, K. J., Specht, C. A., Beeman, R. W., Kanost, M. R., & Muthukrishnan, S. (2004). Characterization of two chitin synthase genes of the red flour beetle, *Tribolium castaneum*, and alternate exon usage in one of the genes during development. Insect biochemistry and molecular biology, 34(3), 291–304. https://doi.org/10.1016/j.ibmb.2003.11.004
- 32. Zhang, X., & Yan Zhu, K. (2013). Biochemical characterization of chitin synthase activity and inhibition in the African malaria mosquito, *Anopheles gambiae*. Insect science, 20(2), 158–166.

- https://doi.org/10.1111/j.1744-7917.2012.01568.x
- 33. Wang, Z., Yang, H., Zhou, C., Yang, W. J., Jin, D. C., & Long, G. Y. (2019). Molecular cloning, expression, and functional analysis of the chitin synthase 1 gene and its two alternative splicing variants in the white-backed planthopper, *Sogatella furcifera* (Hemiptera: Delphacidae). *Scientific reports*, 9(1), 1087. https://doi.org/10.1038/s41598-018-37488-5
- 34. Xu, G., Zhang, J., Lyu, H., Liu, J., Ding, Y., Feng, Q., Song, Q., & Zheng, S. (2017). *BmCHSA-2b*, a Lepidoptera specific alternative splicing variant of epidermal chitin synthase, is required for pupal wing development in *Bombyx mori*. Insect biochemistry and molecular biology, 87, 117–126. https://doi.org/10.1016/j.ibmb.2017.06.017
- 35. Arakane, Y., Dixit, R., Begum, K., Park, Y., Specht, C. A., Merzendorfer, H., Kramer, K. J., Muthukrishnan, S., & Beeman, R. W. (2009). Analysis of functions of the chitin deacetylase gene family in *Tribolium castaneum*. Insect biochemistry and molecular biology, 39(5–6), 355–365. https://doi.org/10.1016/j.ibmb.2009.02.002
- 36. Zhang, T., Huo, Y., Dong, Q., Liu, W., Gao, L., Zhou, J., Li, D., Zhang, X., Zhang, J., & Zhang, M. (2022). *LmCht5-1* and *LmCht5-2* Promote the Degradation of Serosal and Pro-Nymphal Cuticles during Locust Embryonic Development. *Biology*, 11(12), 1778. https://doi.org/10.3390/biology11121778
- 37. Abdel-Banat, B. M., & Koga, D. (2002). Alternative splicing of the primary transcript generates heterogeneity within the products of the gene for *Bombyx mori* chitinase. The Journal of Biological Chemistry, 277(34), 30524–30534. https://doi.org/10.1074/jbc.M112422200
- 38. Ortigão-Farias, J. R., Di-Blasi, T., Telleria, E. L., Andorinho, A. C., Lemos-Silva, T., Ramalho-Ortigão, M., Tempone, A. J., & Traub-Csekö, Y. M. (2018). Alternative splicing originates different domain structure organization of *Lutzomyia longipalpis* chitinases. Memorias do Instituto Oswaldo Cruz, 113(2), 96–101. https://doi.org/10.1590/0074-02760170179
- 39. Vaaje-Kolstad, G., Westereng, B., Horn, S.J., Liu, Z., Zhai, H., Sorlie, M. et al. (2010) An oxidative enzyme boosting the enzymatic conversion of recalcitrant polysaccharides. Science. 330, 219–222. https://doi.org/10.1126/science.1192231
- 40. Couturier, M., Ladeveze, S., Sulzenbacher, G., Ciano, L., Fanuel, M., Moreau, C. et al. (2018) Lytic xylan oxidases from wood-decay fungi unlock biomass degradation. Nature Chemical Biology. 14, 306–310. https://doi.org/10.1038/nchembio.2558
- 41. Forsberg, Z., Sorlie, M., Petrovic, D., Courtade, G., Aachmann, F. L. Vaaje-Kolstad, G. et al. (2019) Polysaccharide degradation by lytic polysaccharide monooxygenases. Current Opinion in Structural Biology. 59, 54–64. https://doi.org/10.1016/j.sbi.2019.02.015
- 42. Sabbadin, F., Urresti, S., Henrissat, B., Avrova Anna, O., Welsh Lydia, R.J., Lindley Peter, J. et al. (2021) Secreted pectin monooxygenases drive plant infection by pathogenic oomycetes. Science. 373, 774–779. https://doi.org/10.1126/science.abj1342
- 43. Tandrup, T., Frandsen, K.E.H., Johansen, K.S., Berrin, J.G. and Lo Leggio, L. (2018) Recent insights into lytic polysaccharide monooxygenases (LPMOs). Biochemical Society Transactions. 46, 1431–1447. https://doi.org/10.1042/BST20170549

- 44. Jagadeeswaran, G., Veale, L., & Mort, A. J. (2021). Do Lytic Polysaccharide Monooxygenases Aid in Plant Pathogenesis and Herbivory. Trends in plant science. 26(2), 142–155. https://doi.org/10.1016/j.tplants.2020.09.013
- 45. Sabbadin, F., Hemsworth, G.R., Ciano, L., Henrissat, B., Dupree, P., Tryfona, T. *et al.* (2018) An ancient family of lytic polysaccharide monooxygenases with roles in arthropod development and biomass digestion. Natural Communications. 9, 756. https://doi.org/10.1038/s41467-018-03142-x
- 46. Zhu, Q., Arakane, Y., Beeman, R. W., Kramer, K. J., and Muthukrishnan, S. (2008) Characterization of recombinant chitinase-like proteins of *Drosophila melanogaster* and *Tribolium castaneum*. Insect biochemistry and molecular biology. 38, 467–477. https://doi.org/10.1016/j.ibmb.2007.06.011
- 47. Franco Cairo, J. P. L., Cannella, D., Oliveira, L. C., Gonçalves, T. A., Rubio, M. V., Terrasan, C. R. F., Tramontina, R., Mofatto, L. S., Carazzolle, M. F., Garcia, W., Felby, C., Damasio, A., Walton, P. H., & Squina, F. (2021). On the roles of AA15 lytic polysaccharide monooxygenases derived from the termite Coptotermes gestroi. Journal of inorganic biochemistry, 216, 111316. https://doi.org/10.1016/j.jinorgbio.2020.111316
- 48. Dong, Z., Zhang, W., Zhang, Y., Zhang, X., Zhao, P. and Xia, Q. (2016) Identification and characterization of novel chitin-binding proteins from the larval cuticle of Silkworm, Bombyx mori. Journal of Proteome Research. 15, 1435–1445. https://doi.org/10.1021/acs.jproteome.5b00943

Figures

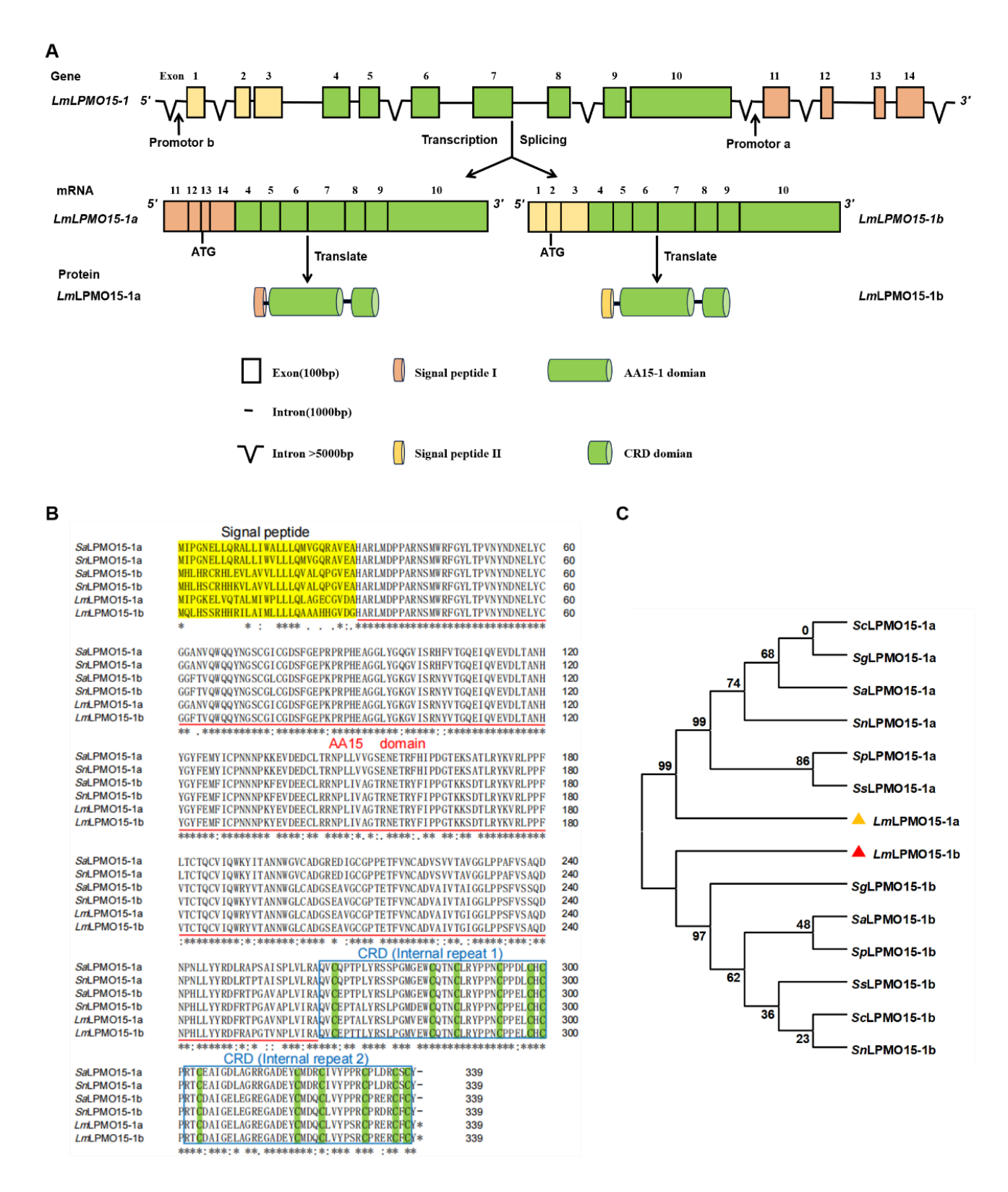
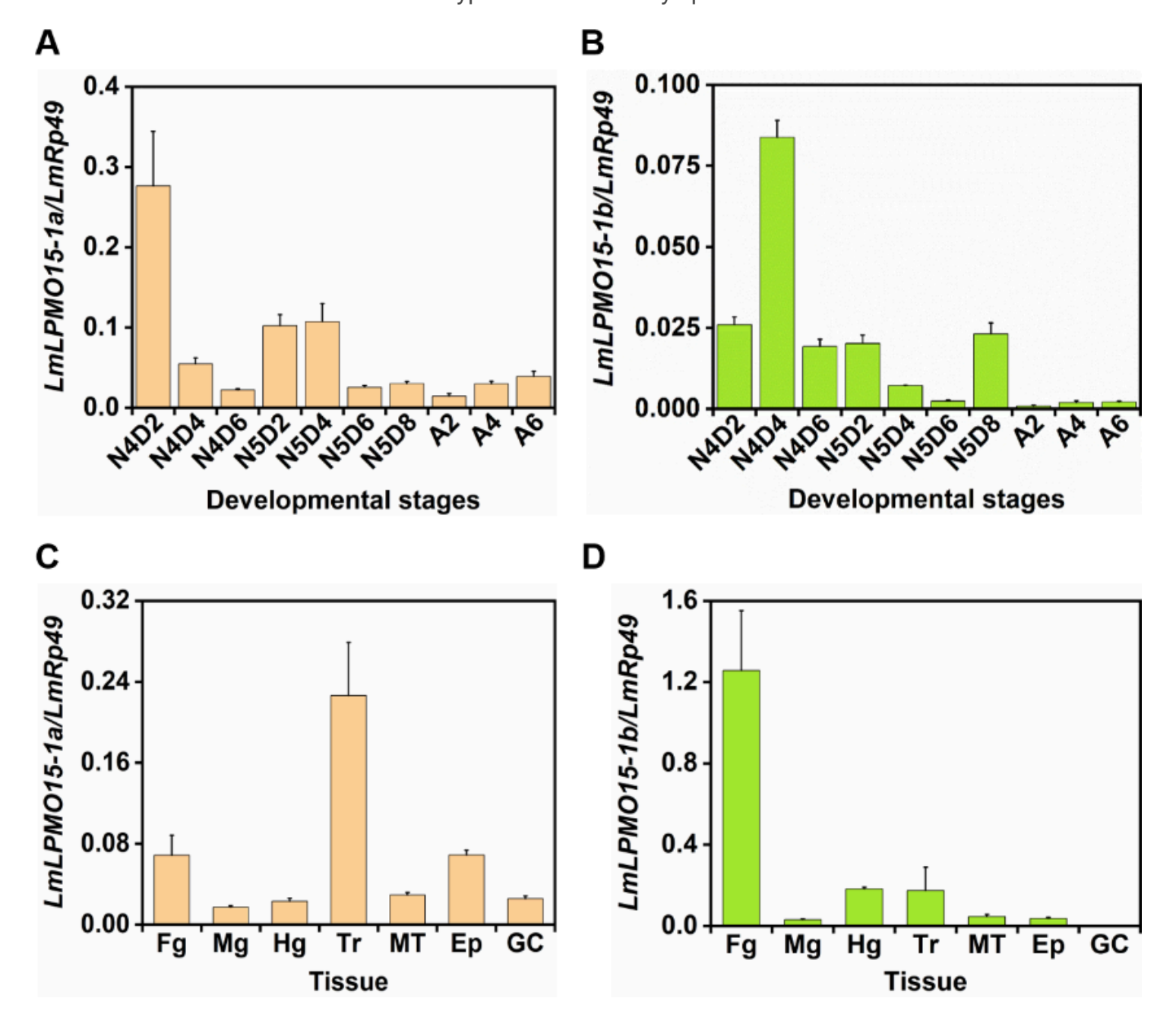


Figure 1

Gene structure and phylogenetic analyses of *LmLPMO15-1*. A Exon-intron structure, alternative splicing pattern, and translated protein structure organization of *LmLPMO15-1a* and *LmLPMO15-1b*. Rectangles and black lines represent exons and introns, respectively. Yellow and orange rectangles denote splicing exons, while green rectangles represent exons shared by two transcripts. The translated proteins of *LmLPMO15-1a* and *LmLPMO15-1b* differ only in the signal peptide, indicated as Signal Peptide I (orange)

and Signal Peptide II (yellow), respectively. **B** Amino acid sequence alignment of *Lm*LPM015-1s. Predicted signal peptides are highlighted in yellow. The AA15 domain is indicated by the red underline. The conserved cysteine residues at the C-terminus are highlighted in green. The conserved Cysteine-Rich Domain (CRD) with an unknown function is indicated in Blue boxes. **C** The phylogenetic tree was constructed using the signal peptide sequences of orthopteran LPM015-1s. It was constructed using the neighbor-joining method in MEGA 11. *Lm*LPM015-1a and *Lm*LPM015-1b are marked with red and orange triangles, respectively. Values at cluster branches indicate the results of the bootstrap analysis. GenBank accession numbers of the two types of alternatively spliced variants were listed in Table S2.



Gene expression patterns of *LmLPMO15-1a* and *LmLPMO15-1b* in *L. migratoria*. Stage-specific expression pattern of *LmLPMO15-1a* (A) and *LmLPMO15-1b* (B). Tissue-specific expression patterns of

Figure 2

LmLPMO15-1a (**C**) and LmLPMO15-1b (**D**). To detect the stage-specific expression pattern, the fourth instar day-2 (N4D2), fourth instar day-4 (N4D4), fourth instar day-6 (N4D6), fifth instar day-2 (N5D2), fifth instar day-4 nymph (N5D4), fifth instar day-6 (N5D6), fifth instar day-8 (N5D8) nymphs, and day-2 (A2), day-4 (A4), day-6 (A6) adults were collected. The foregut (Fg), midgut (Mg), hindgut (Hg), trachea (Tr), malpighian tubules (MT), epidermis (Ep), and gastric caecum (GC) were dissected from L. migratoria on the fifth instar day-3, to detect the tissue-specific expression pattern. Total RNA was extracted from these samples for RT-qPCR analysis. The housekeeping gene LmRp49 was used as a reference gene. The relative expression levels for each gene were calculated relative to those of the reference gene LmRp49 according to the $2^{-\Delta\Delta Ct}$ method. Each sample included three biological replicates and three technical replicates.

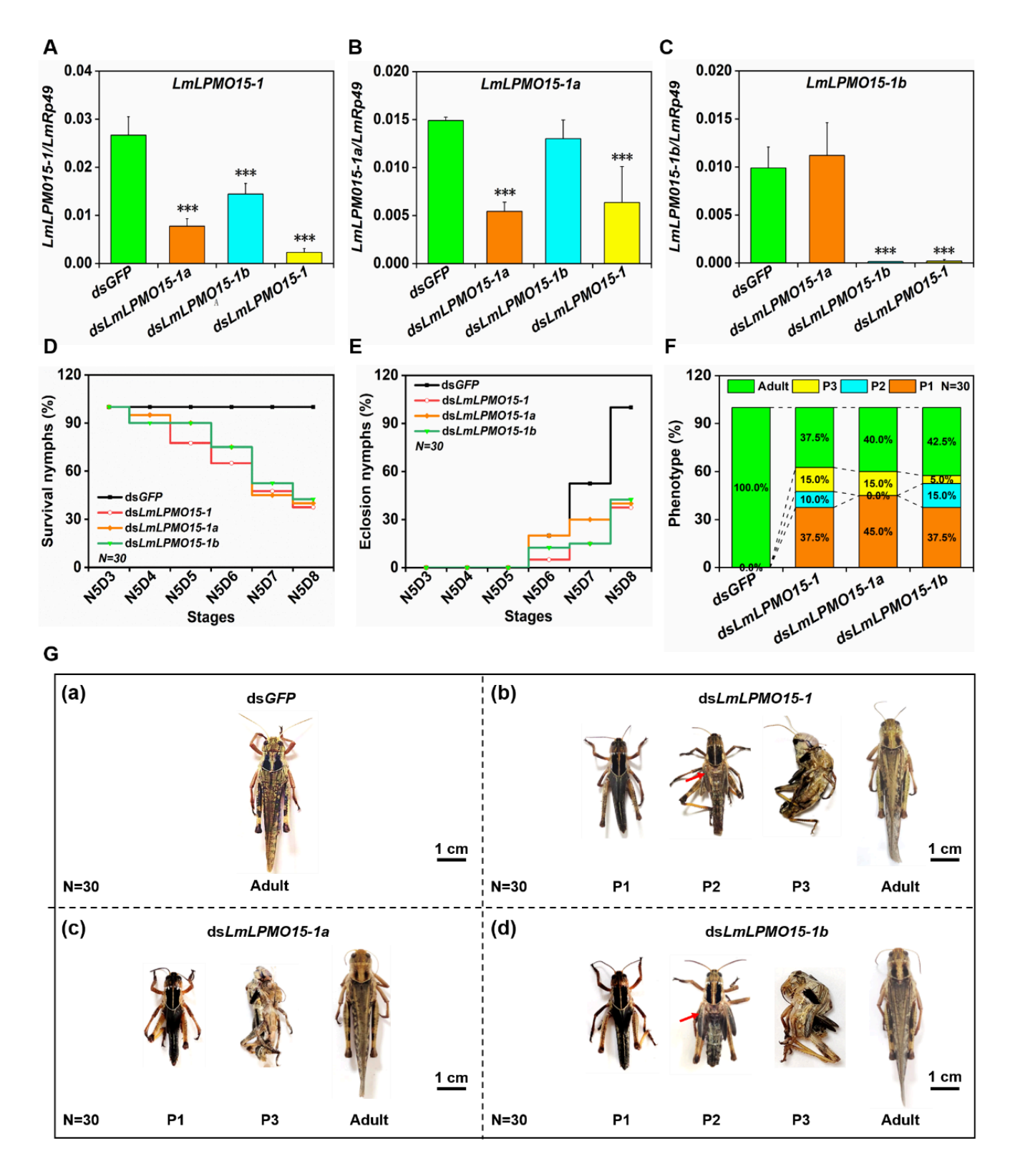
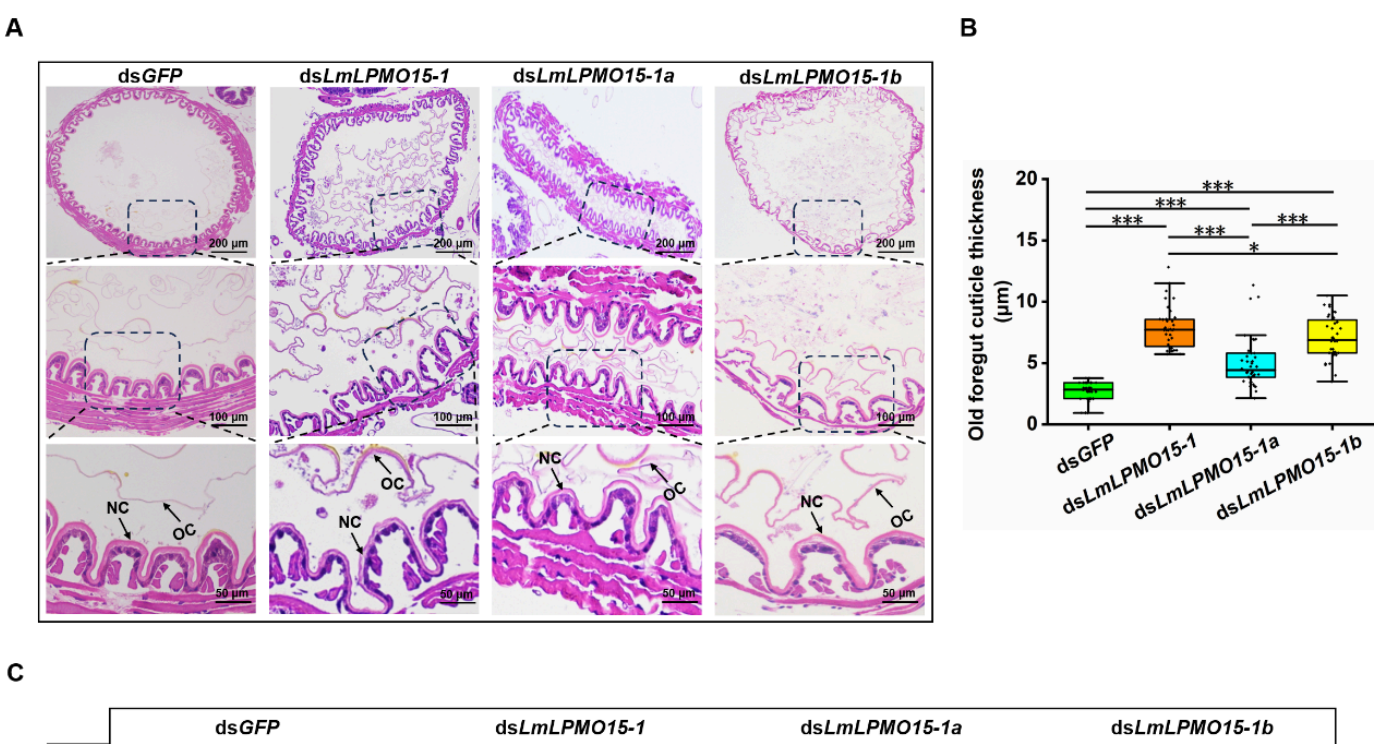


Figure 3

The effect of ds*LmLPMO15-1*,ds*LmLPMO15-1a*, and ds*LmLPMO15-1b* injection during the nymph-adult molt. A-C Silencing efficiency determined at 24 h after injection of ds*LmLPMO15-1*, ds*LmLPMO15-1a*, or ds*LmLPMO15-1b*. The transcript level of the reference gene *LmRP49* was used to normalize transcript levels of *LmLPMO15-1s*. Data represented the means ± SE of three independent biological replications. Statistical significance was analyzed with Student's t-test (*, P<0.05, ***, P<0.01. ****, P<0.001). **D-E**

Survival and eclosion rate of *L. migratoria* after ds*LmLPMO15-1a*, ds*LmLPMO15-1b*, or ds*LmLPMO15-1* injection. **F-G** Phenotypes and Percentage of each phenotype of *L. migratoria* after the injection of ds*LmLPMO15-1*, ds*LmLPMO15-1a*, ds*LmLPMO15-1b*, or ds*GFP* (control). All of the locusts injected with ds*GFP* were able to molt to the adult stage successfully. Upon injecting ds*LmLPMO15-1*, ds*LmLPMO15-1a*, or ds*LmLPMO15-1b*, the locusts exhibited four phenotypes types characterized by successful molt into the adult, arrested development and death before molting (P1), molt failure phenotype with just-expanded wing (P2), and a molt failure phenotype exhibiting a more advanced molt (P3). P1 to P3 indicate three lethal phenotypes.



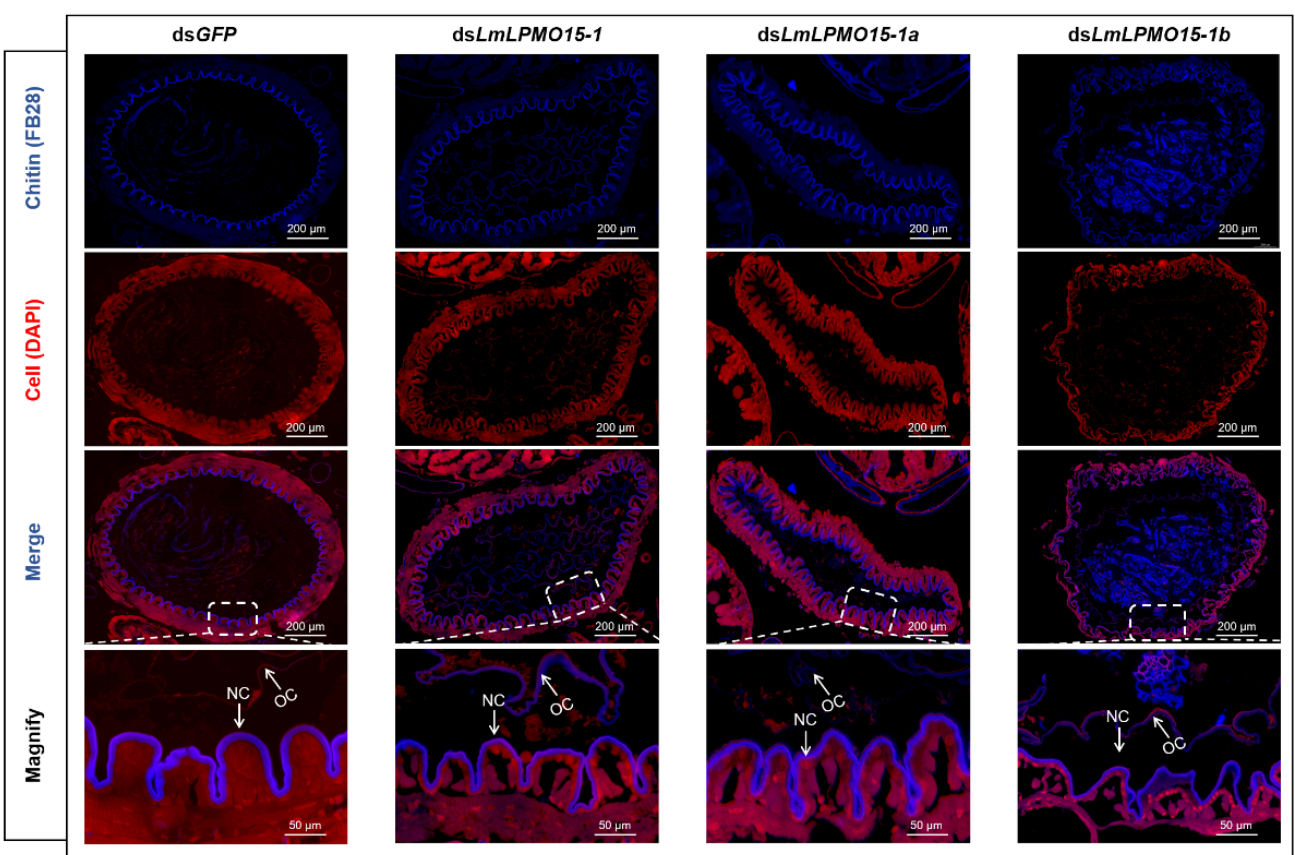


Figure 4

Observation of the foregut (proventriculus) structure after dsRNA injection in L. migratoria. A

Hematoxylin and eosin staining of the paraffin sections (5 μ m) of foregut from the fifth instar day-8 nymphs (molting stage) injected with different dsRNAs. **B** The thickness of old foregut cuticle in *L. migratoria* injected with different dsRNAs. They were then imaged using an Olympus IX-83 inverted

fluorescence microscope. OC, old cuticle; NC, new cuticle. Statistical significance was analyzed with Student's t-test (*, P<0.05; **, P<0.01; ***, P<0.001).

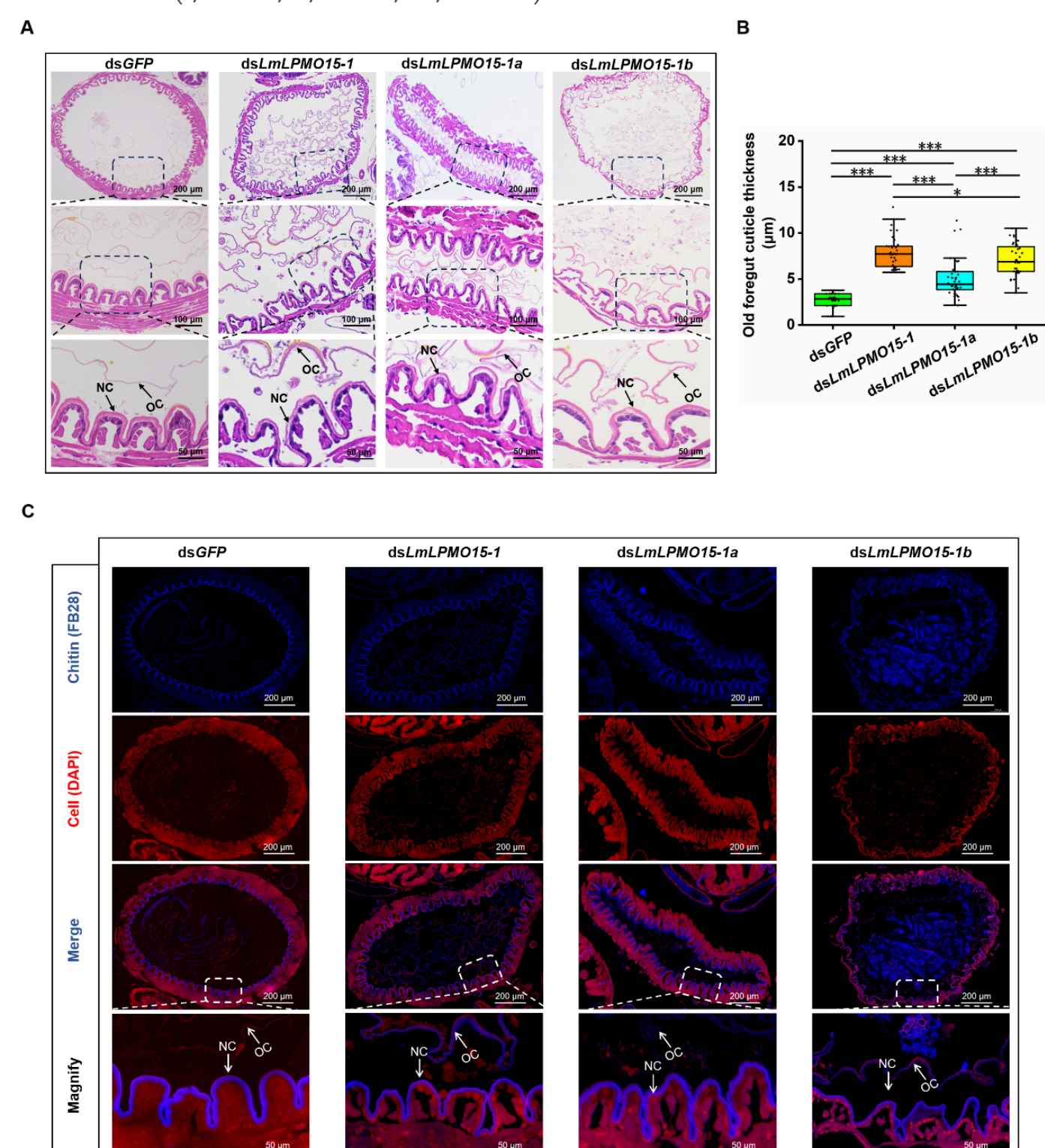


Figure 5

Observation of the foregut (proventriculus)structure after dsRNA injection in *L. migratoria* by fluorescence staining. Fluorescent Brightener 28 (FB28) was used to restain chitin (in blue) in paraffin

sections of the proventriculus, while DAPI was employed to restain cell nuclei (in red). They were then imaged using an Olympus IX-83 inverted fluorescence microscope. OC, old cuticle; NC, new cuticle.

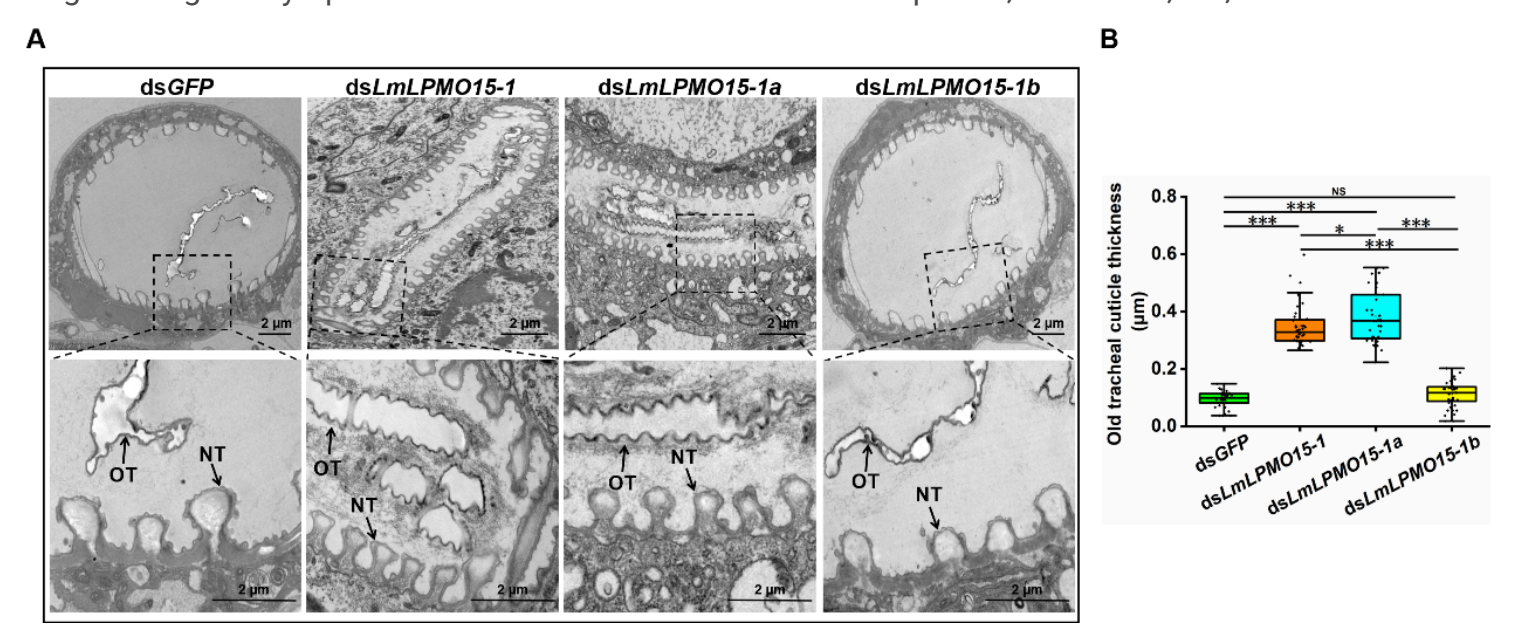


Figure 6

Observation of tracheal structure by Transmission Electron Microscopy after RNAi of *LmLPMO15-1s*. A Morphological observation of the trachea after RNAi by TEM. N5D8 nymphs (molting stage) injected with dsRNA were embedded in resin and sectioned for observation. OT, old tracheal cuticle; NT, new tracheal cuticle; Scale bar = 2μ m. **B** The thickness of old tracheal cuticle after RNAi. Statistical significance was analyzed with Student's t-test (*, P<0.05, **, P<0.01. ***, P<0.001, NS, No significant difference).